

Induction of apoptosis by total flavonoids from *Scutellaria barbata* D. Don in human hepatocarcinoma MHCC97-H cells via the mitochondrial pathway

Jie Gao · Wang-Feng Lu · Zhi-Jun Dai · Shuai Lin · Yang Zhao · Sha Li · Nuan-Nuan Zhao · Xi-Jing Wang · Hua-Feng Kang · Xiao-Bin Ma · Wang-Gang Zhang

Received: 16 September 2013 / Accepted: 14 October 2013 / Published online: 13 November 2013
© International Society of Oncology and BioMarkers (ISOBM) 2013

Abstract *Scutellaria barbata* D. Don, a traditional Chinese medicine, reportedly possesses antitumor activity against a variety of tumors. In the present study, we investigated the cytotoxic effect of total flavonoids from *S. barbata* (TF-SB) on human hepatocarcinoma cells and the underlying molecular mechanisms regarding the effect were explored. TF-SB treatment significantly reduced the cell viability of human HCC MHCC97-H cells in a dose-dependent manner. Further flow cytometric analysis showed that the apoptosis

rate of MHCC97-H cells increased and the mitochondrial membrane potential ($\Delta\psi_m$) of MHCC97-H cells decreased after TF-SB treatment. DNA ladder showed that TF-SB induced a significant increase in DNA fragmentation in MHCC97-H cells. Reverse transcription PCR and Western blot analysis revealed that the expression levels of Smac, Apaf-1, Cytochrome c, Caspase-9, and Caspase-3 were upregulated in a dose-dependent manner and after treatment with different concentrations of TF-SB for 48 h. These results suggest that TF-SB induces apoptosis in MHCC97-H cells through the mitochondrial pathway.

J. Gao and W.-F. Lu contributed equally to this work.

J. Gao · W.-F. Lu · Z.-J. Dai (✉) · S. Lin · Y. Zhao · X.-J. Wang · H.-F. Kang · X.-B. Ma
Department of Oncology, The Second Affiliated Hospital of Xi'an Jiaotong University, Xi'an 710004, China
e-mail: dzj0911@126.com

J. Gao
Department of Nephrology, The Second Affiliated Hospital of Xi'an Jiaotong University, Xi'an 710004, China

W.-F. Lu
Department of Surgical Oncology, Shangluo Central Hospital, Shangluo 726000, China

S. Li · N.-N. Zhao
Department of Pharmacology, The Second Affiliated Hospital of Xi'an Jiaotong University, 710004 Xi'an, China

W.-G. Zhang (✉)
Department of Hematology, The Second Affiliated Hospital of Xi'an Jiaotong University, Xi'an 710004, China
e-mail: zwgang2013@126.com

Keywords *Scutellaria barbata* · Hepatocarcinoma · Apoptosis · Mitochondrial

Abbreviations

HCC	Hepatocellular carcinoma
TF-SB	Total flavones of <i>Scutellaria barbata</i>
$\Delta\psi_m$	Mitochondrial membrane potential
MTT	3-(4,5-Dimethylthiazol-2-yl)-2,5-diphenyl tetrazolium bromide
DMEM	Dulbecco's modified Eagle's medium
Smac	Second mitochondria-derived activator of caspase
Apaf-1	Apoptotic protease activating factor
RT-PCR	Reverse transcription polymerase chain reaction
HPLC	High-performance liquid chromatography
PI	Propidium iodide
FCM	Flow cytometry

Introduction

Hepatocellular carcinoma (HCC) is one of the most common malignancies with an estimated 695,900 cancer-related deaths worldwide [1]. Currently, multidisciplinary treatment significantly improves efficacy among the patients with advanced HCC. However, recurrence and metastasis are still the leading causes of patient death [2]. Multiple therapeutic approaches, including surgical resection, liver transplantation, transarterial chemoembolization, and chemotherapy, are of limited efficacy in Chinese patients with HCC [3]. Therefore, researchers have focused on the potential development of natural compounds for anticancer therapy [4]. Some extracts from Chinese herbs such as vinblastine, camptothecin, and β -elemene, have been widely used in treating a variety of human cancers [5–7].

Scutellaria barbata D. Don is one of the traditional herbs and is widely distributed in southern China [8]. *S. barbata* extract (SBE) has in vitro growth inhibitory effects on a variety of tumors, such as liver cancer, colorectal cancer, lung cancer, and breast cancer [9–12]. However, its antitumor mechanism is still unknown. The antitumor activity of herbs is closely related to apoptotic activation [13]. Apoptosis is a major pathway for maintaining the steady-state cells [14]. Recent studies have shown that apoptosis presents through a death receptor pathway, a mitochondria pathway, and an endoplasmic reticulum stress-mediated pathway [15–17], in which mitochondria play a key role in apoptosis [18]. The mitochondrial pathway initiates apoptosis through the regulation of many proteins. These regulatory proteins usually change mitochondrial membrane permeability and decrease the mitochondrial membrane potential ($\Delta\psi_m$), thereby in turn inducing the release of cytochrome C and mitochondrion-dependent caspase activation as a result to apoptosis triggering [19, 20].

To date, several flavonoids, alkaloids, polysaccharides, and steroids from *S. barbata* have been characterized [21]. In this study, we focused on the mechanism underlying the anticancer effects of total flavonoids of *S. barbata* (TF-SB) on HCC cells in vitro, with the emphasis on alterations in $\Delta\psi_m$ and apoptosis induction. We found that TF-SB induces the apoptosis of MHCC97-H cells through the mitochondrial dysfunction pathway.

Materials and methods

Cell line, cell culture, and reagents

HCC cell line MHCC97-H was obtained from the Shanghai Institute of Cell Biology Cells maintained in Dulbecco's

modified Eagle's medium (DMEM) supplemented with 10 % v/v fetal bovine serum (FBS), and 100 μ g/mL penicillin/streptomycin at 37 °C in a humidified atmosphere containing 5 % CO₂.

DMEM and FBS were purchased from Gibco, Life Technologies (Carlsbad, CA, USA). Trypsin-EDTA, penicillin, streptomycin, dimethyl sulfoxide (DMSO), 3-(4,5-dimethylthiazol-2-yl)-2,5-diphenyltetrazolium bromide (MTT) were from Sigma-Aldrich (St. Louis, MO, USA). The dual-emission potential-sensitive probe 5,5',6,6'-tetra-chloro-1,1',3,3'-tetraethyl-imidacarbocyanine iodide (JC-1) was from Beyotime Institute of Biotechnology (Shanghai, China). Reverse transcription polymerase chain reaction (RT-PCR) kit (catalog no. sc-8319) was from Ampliqon A/S (Odense, Denmark), Trizol was from Invitrogen, USA, and TIANamp Genomic DNA kit was from Beijing, China. Antibodies against second mitochondria-derived activator of caspase (Smac), apoptotic protease activating factor (Apaf-1), cytochrome c, caspase-9, caspase-3, and β -actin were purchased from Santa Cruz Biotechnology (Santa Cruz, CA, USA). Peroxidase-conjugated antibodies against mouse IgG or rabbit IgG were purchased from Abgent (San Diego, CA, USA).

Preparation of TF-SB from *Scutellaria barbata* D. Don

Dried plant materials of *S. barbata* were purchased from Yi Shan Tang Chinese Herbal medicine store (Xi'an, China) and authenticated according to the descriptions found in the Chinese Pharmacopoeia. The original herb was identified as *S. barbata* D. Don (SB) by Run-Xia Liu at the Medical School of Xi'an Jiaotong University (Xi'an, China). The voucher samples, ZLK-ZY-05 (*S. barbata*), were deposited at the Department of Oncology, the Second Affiliated Hospital of Xi'an Jiaotong University.

The material was coarsely ground before extraction. A total of 300 g of the material was extracted twice with 95 % ethanol for 3 h in 50 °C. The infusion was filtered through a 1-mm pore-size filter. The leftover was collected after the combined extracts evaporated. The pH of *S. barbata* sample extract was adjusted to 2.0, and then the crude extract was chromatographed on an AB-8 macroporous adsorption resin column. After being eluted with 3 multiple column volume of distilled water and 12 multiple column volume of 70 % ethanol, the flavonoids purity increased with a recovery of 69 % [21]. The total flavonoids were stored at 4 °C for use.

High-performance liquid chromatography analysis

The components of TF-SB were identified using high-performance liquid chromatography (HPLC). An accurately weighed 100 mg TF-SB was dissolved in 50 mL methanol for HPLC analysis. For chromatographic analysis, Agilent Zorbax C18 column (5 μ m, 250 \times 4.6 mm) with a guard column (C18, 5 μ m, 4.0 \times 3.0 mm) was used. HPLC separation was performed using a linear gradient with a flow rate of 1.0 mL/min, while column was kept in an insulated compartment at 30 $^{\circ}$ C. The mobile phase consisted of water containing 1.0 % acetic acid (A) and acetonitrile (B) using a gradient of 28–80 % B for 0–60 min. The injection volume was 10 μ L. The UV detection wave length was set at 280 nm.

Assessment of cell viability

Cells were seeded in a 96-well plate at a density of 1×10^4 cells/well and cultured with serum-free DMEM for 12 h, and then treated with different concentrations of TF-SB (0, 30, 60, 120, and 240 μ g/mL) for 24, 48, and 72 h at 37 $^{\circ}$ C and 5 % CO₂. After treatment, the medium was aspirated, and 20 μ L of MTT (Sigma) was added to each well and incubated for 4 h, and then, 150 μ L of DMSO (Sigma) was added to each well. After shaking the plate for 10 min, the optical density (OD) was measured at 490 nm using an enzyme-labeling instrument (EX-800 type, Bio-Tek, Winooski, VT, USA). The cell viability was determined according to the following formula: Cell viability (%) = OD of sample \times 100 / OD of control.

Measurement of apoptosis

Detection of apoptotic cells were performed using double staining of annexin V-FITC and propidium iodide (PI) (BD Biosciences, USA). MHCC97-H cells (1×10^6 cells/mL) were plated and treated with different concentrations of TF-SB in for 48 h. The cells were harvested and washed twice with 4 $^{\circ}$ C phosphate-buffered saline (PBS). The samples were resuspended with 500 μ L of 1 \times binding buffer in the labeled tube; 5 μ L of annexin V-FITC and 10 μ L PI were added into the labeled tube and stained with annexin V and PI for 20 min at room temperature in the dark. The samples were analyzed using flow cytometry (FCM) analysis (BD Biosciences Clontech, USA). This experiment was repeated for three times.

DNA ladder assay

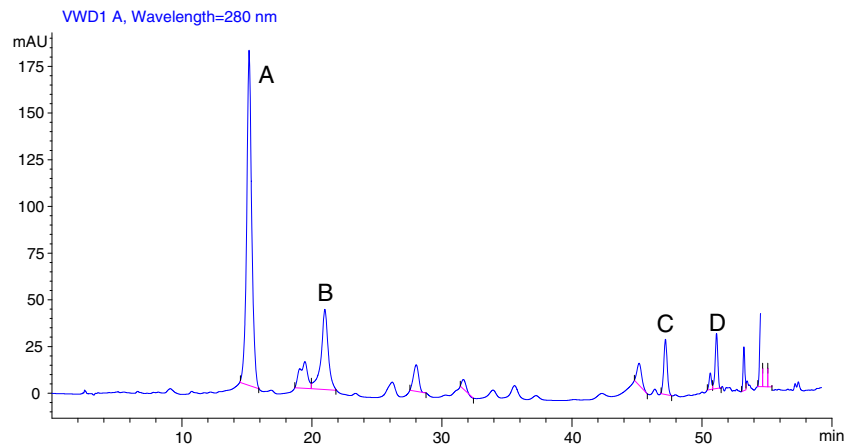
MHCC97-H cells were collected after 24 h of treatment with TF-SB (30, 60, and 90 μ g/mL). DNA ladder extraction was performed using a TIANamp Genomic DNA kit (Beijing, China). The cells were lysed for 2 h in a solution containing 10 mM Tris-HCl (pH 7.8), 1 mM ethylenediaminetetraacetic acid (EDTA), 10 mM NaCl, 1 % sodium dodecyl sulfate (SDS), and 1 mg/mL proteinase K at 56 $^{\circ}$ C, and treated with 10 mg/mL RNase A for an additional 60 min at 37 $^{\circ}$ C. The lysate was extracted twice with phenol-chloroform (1:1 v/v) and precipitated overnight with ethanol at -20 $^{\circ}$ C. The precipitate was washed twice in 70 % ethanol and finally dissolved in 100 μ L of TE (1 mM EDTA, 10 mM Tris-HCl, pH 8.0). The resulting DNA (10 μ L) was loaded onto 2 % agarose gel and electrophoresed, and then the DNA fragments were then photographed. This assay was done triplicate.

Table 1 Primer sequences and annealing temperature of Smac, Apaf-1, cytochrome c, caspase-9, caspase-3, and β -actin in RT-PCR

Gene	Gene sequences	Size (bp)	Annealing temperature ($^{\circ}$ C)
Smac	Forward primer 5'-CTGTGACGATTG GCTTTG-3'	293	54
	Reverse primer 5'-CTCATTCTCTGGC GGTAT-3'		
Apaf-1	Forward primer 5'-TTGCTGCCCTTC TCCATGAT-3'	285	59
	Reverse primer 5'-TCCCAACTGAAA CCAATGC-3'		
Cytochrome c	Forward primer 5'-GAGCGGGAGTGT TCGTTGT-3'	327	59
	Reverse primer 5'-GTCTGCCCTTTC TTCCTTCT-3'		
Caspase-3	Forward primer 5'-CATCCAGTCGCT TTCTGCC-3'	623	60
	Reverse primer 5'-TGCCCACAGATG CCTAAGTTC-3'		
Caspase-9	Forward primer 5'-CGAACTAACACG CAAGCA-3'	142	56
	Reverse primer 5'-CAAATCCTCCAG AACCAAT-3'		
β -actin	Forward primer 5'-CGGGACCTGACT GACTACCTC-3'	549	61
	Reverse primer 5'-GCACTCGTGATA CTCCTGCTTG-3'		

The primer pairs and the predicted sizes of the amplified PCR products and the annealing temperatures of PCR are listed. β -Actin is the housekeeping gene for RT-PCR analysis. The primer sequences were designed with Primer Premier 5.0 software

Fig. 1 HPLC analysis of TF-SB. There was a main peak in HPLC, which was identified as scutellarin (*A*). There were also some other flavonoids in TF-SB, which were identified as apigenin (*B*), baicalein (*C*), and luteolin (*D*) (wavelength=280 nm)



Measurement of mitochondrial membrane potential ($\Delta\psi_m$)

According to the instructions of JC-1 Mitochondrial Apoptosis Detection Kit, JC-1 accumulated within intact mitochondria to form red-fluorescent J-aggregates at higher membrane potentials and green-fluorescent monomers at low membrane potentials [22]. The MHCC97-H cells were harvested with and without 48 h of TF-SB treatment. The cells were adjusted to a concentration of 1×10^5 cells/mL and incubated with 500 μ L (2 mg/L) JC-1 working solution for 20 min at 37 °C. Then, the supernatant was discarded and washed twice with $1 \times$ JC-1 buffer. The samples were resuspended with 500 μ L of $1 \times$ JC-1 buffer and were analyzed afterwards using FCM.

Reverse transcription polymerase chain reaction

MHCC97-H cells were seeded in six-well plate and treated with concentration TF-SB (0, 30, 60, and 90 μ g/mL) separately for 48 h. Total cellular RNA was extracted using the Trizol reagent following the manufacturer's instructions. Polymerase chain reaction was carried out using specific sense and antisense PCR primers for amplification. The primer sequences were designed with Primer Premier 5.0 software (Premier Biosoft, Palo Alto, CA, USA). The primer sequences and annealing temperature of the genes are shown in Table 1. PCR product was detected on 2 % agarose gel electrophoresis and ethidium bromide staining, and was used the gray analysis by imaging system. The expression intensity of destination gene messenger RNA (mRNA) was denoted with the ratio of the photodensity of the RT-PCR products of destination gene and β -actin.

Western blot analysis

After treated with different concentrations (0, 30, 60, and 90 μ g/mL) of TF-SB for 48 h, the cells were rinsed and lyzed following extract the total protein (BCA protein assay, Pierce, USA). The proteins were transferred by a SDS-polyacrylamide gel and blocked with 5 % nonfat milk in PBS for 2 h. The blotted membranes were incubated with Smac, Apaf-1, cytochrome c, caspase-9, caspase-3, and β -actin antibody (Santa Cruz, CA, USA) with an overnight incubation at 4 °C. The blots were washed three times, and then incubated with secondary antibodies conjugated with horseradish peroxidase (1:1,000; Santa

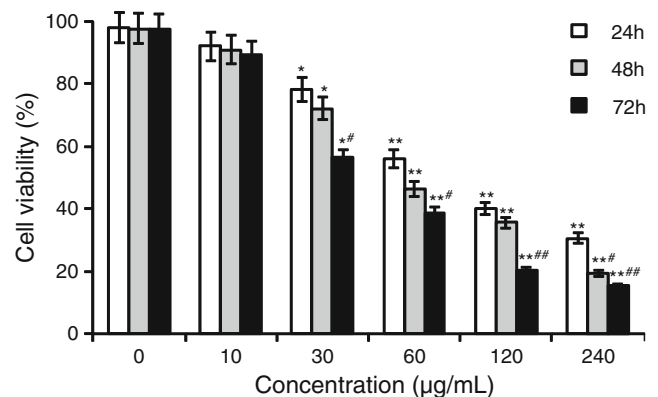


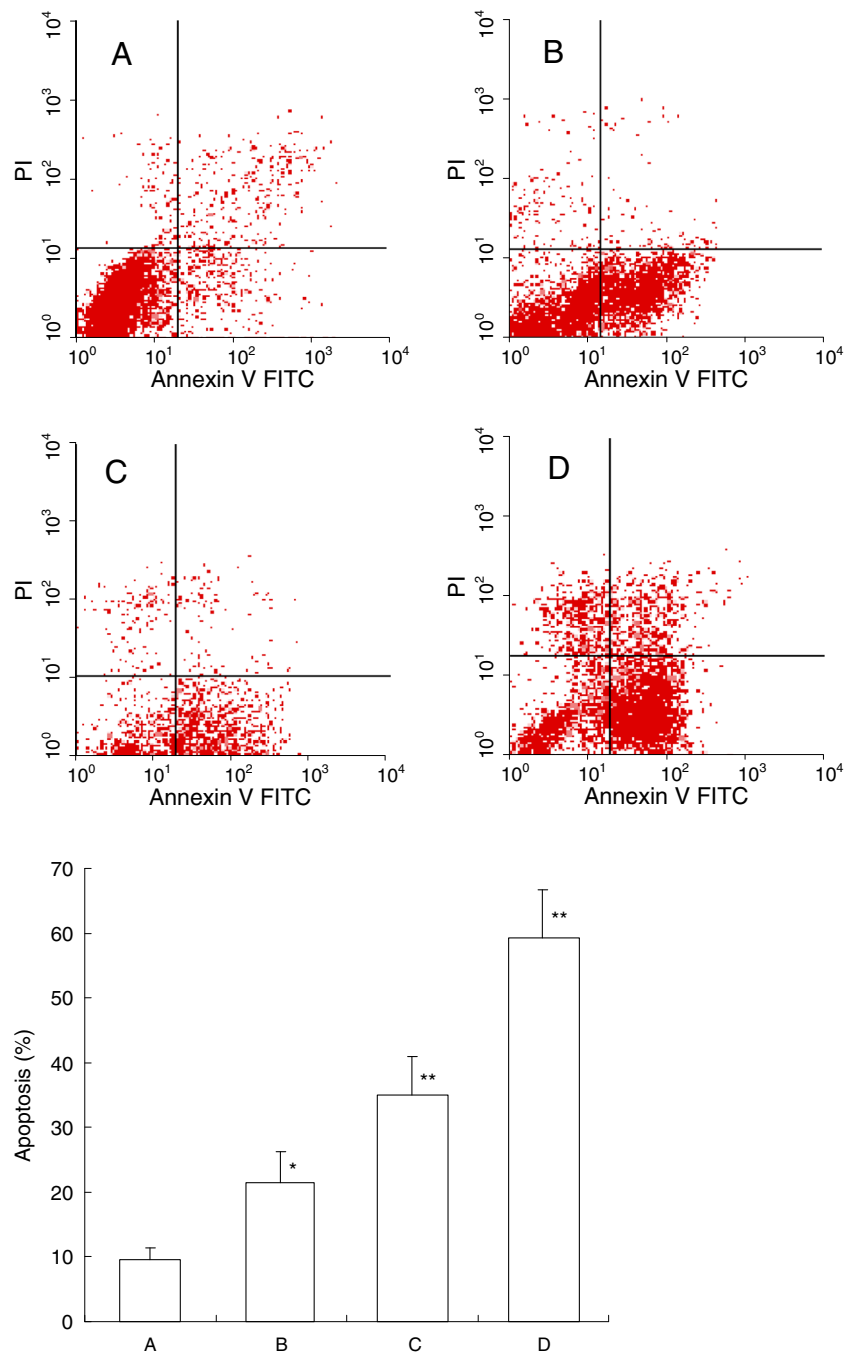
Fig. 2 TF-SB efficiently attenuated the viability of MHCC97-H cells. Cells were treated with the different concentrations of TF-SB (10, 30, 60, 120, and 240 μ g/mL) of TF-SB for 24, 48, and 72 h. Cell viability was determined by MTT assay. This assay was triplicated for mean \pm SEM. Dose and time dependence of cell growth could be elucidated by ANOVA analysis. * $P < 0.05$, ** $P < 0.01$ compared with 0 μ g/mL TF-SB; # $P < 0.05$, ## $P < 0.01$ compared with 24 h

Cruz Biotechnology). After washed three times by PBS, the immunoblotting signals were developed by ECL chemiluminescence. Photographs were taken, and optical densities of the bands were scanned and quantified with the Gel Doc 2000 (Bio-Rad).

Statistical analysis

The data are presented as the means \pm SEM of at least three independent experiments and analyzed via one-way ANOVA and Student's *t* test using the SPSS 14.0 software.

Fig. 3 TF-SB treatment induces dose-dependent apoptosis in MHCC97-H Cells. Cells treated with various concentrations of TF-SB were double-stained with annexin V and PI and analyzed by FCM. The data are represented as mean \pm SEM from three independent experiments. A control group, B 30 $\mu\text{g}/\text{mL}$ TF-SB group, C 60 $\mu\text{g}/\text{mL}$ TF-SB group, D 90 $\mu\text{g}/\text{mL}$ TF-SB group. * $P < 0.05$, ** $P < 0.01$ compared with the control group



Differences with $P < 0.05$ were considered statistically significant.

Results

Identification of TF-SB by HPLC

The components of TF-SB were identified using HPLC. As shown in Fig. 1, the main peak was identified as scutellarin (A). Other identified flavonoids in TF-SB included apigenin (B), baicalein (C), and luteolin (D). The contents of flavonoids A–D were 67.2, 8.7, 4.6, and 4.3 %, respectively.

TF-SB inhibited the cell viability of MHCC97-H cells

The cells were treated with different TF-SB concentrations (10 to 240 $\mu\text{g/mL}$) as time indicated in the figure. MTT assay was used to examine the antiproliferative effect of TF-SB. The effects of TF-SB on cell growth over 72 h are shown in Fig. 2. The MTT assay showed that TF-SB significantly decreased cell viability in a dose- and time-dependent manner in MHCC97-H cells.

Assessment of apoptosis of MHCC97-H cells using FCM

After treatment with different doses of TF-SB for 48 h, apoptosis induction was observed. According to flow cytometric analysis, apoptotic cells were separated from viable or necrotic ones by combined annexin V-FITC and PI staining. As shown in Fig. 3, in TF-SB groups, the rate of apoptotic cells was gradually increased accompanied with increasing concentrations of TF-SB. By contrast, viable apoptotic cells were rarely detected in the control group. The rate of apoptosis in the control and (30, 60, and 90 $\mu\text{g/mL}$) TF-SB groups were $(9.53 \pm 2.26)\%$, $(21.48 \pm 3.74)\%$, $(34.92 \pm 2.17)\%$, and $(59.22 \pm 4.68)\%$, respectively. The results revealed that apoptotic cells gradually increased in a dose-dependent manner.

TF-SB induced DNA degradation in MHCC97-H cells

DNA was extracted from MHCC97-H cells and subjected to DNA ladder analysis after 48 h of TF-SB treatment. As shown in Fig. 4, the results suggested that TF-SB significantly increased fragmented DNA sequence in a dose-dependent manner.

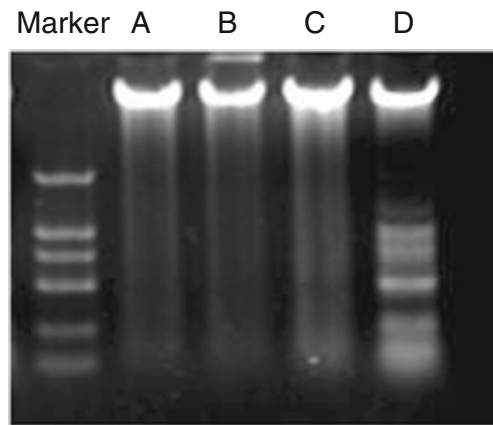


Fig. 4 DNA ladder diagram after treatment with different concentrations of TF-SB for 48 h. *A* blank control group, *B* 30 $\mu\text{g/mL}$ TF-SB group, *C* 60 $\mu\text{g/mL}$ TF-SB group, *D* 90 $\mu\text{g/mL}$ TF-SB group

TF-SB produced a great effect on $\Delta\psi_m$

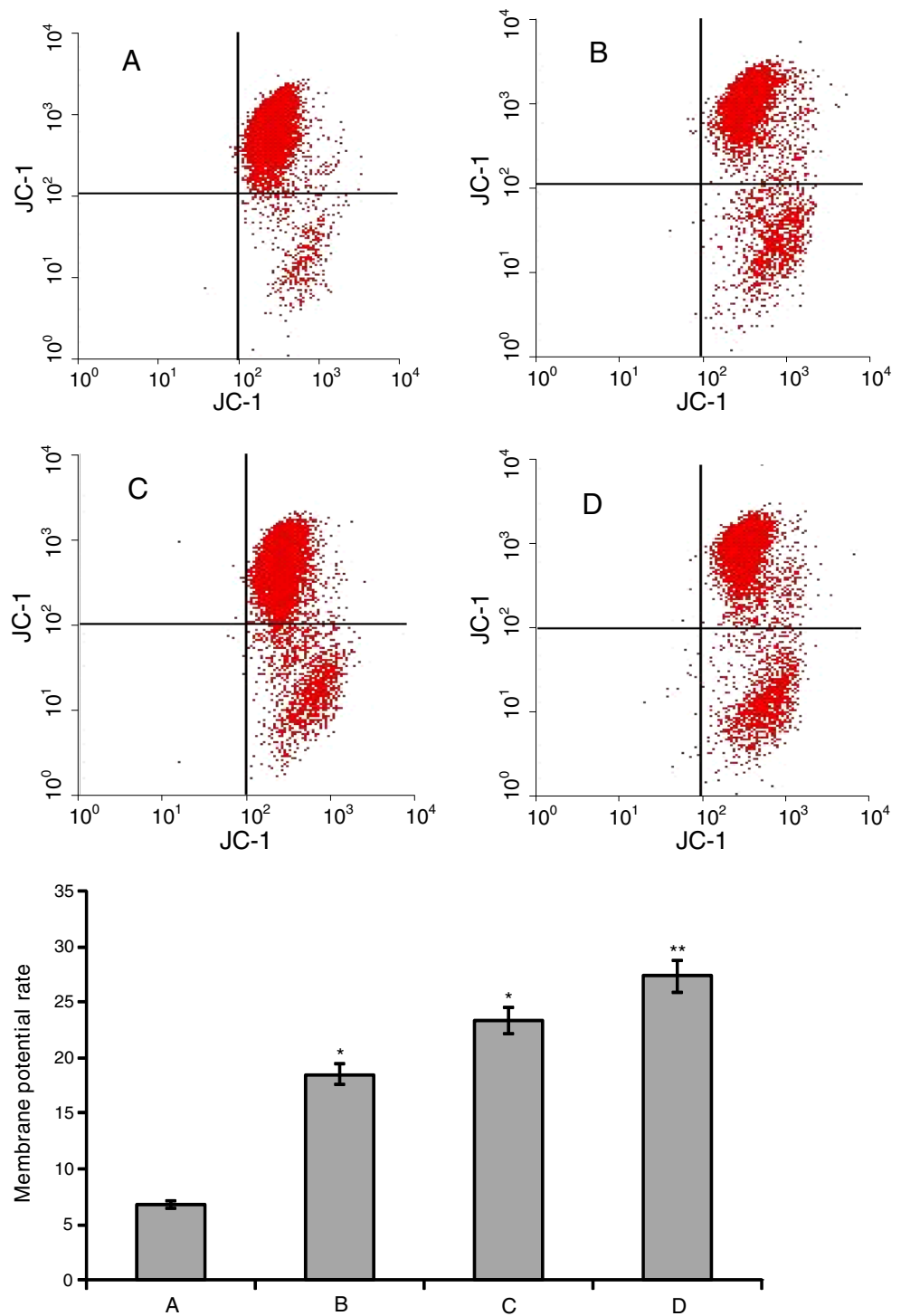
Mitochondria play an essential role in apoptosis. JC-1 is an indicator commonly used for detecting the $\Delta\psi_m$, and it is very sensitive to monitor the membrane potential [22]. In the present study, $\Delta\psi_m$ was detected using FCM via JC-1 staining. As shown in Fig. 5, JC-1 staining showed that $\Delta\psi_m$ decreased with increasing TF-SB concentration. After TF-SB treatment for 48 h, the percentage of depolarized cells (lower quadrants) significantly increased from $18.52 \pm 2.03 \%$ to $27.31 \pm 1.25 \%$ ($P < 0.05$) as compared with the corresponding control ($6.84 \pm 2.27 \%$).

Detection of the mRNA expression of Smac, Apaf-1, caspase-9, and survivin using an RT-PCR assay

Smac plays a crucial role in the mitochondrial apoptosis pathway, and it promotes chemotherapy-induced apoptosis [23]. Apaf1 is the main component of the apoptosome and is a crucial factor in the mitochondria-dependent death pathway [24].

To confirm that TF-SB induces apoptosis via the mitochondrial pathway, the expression levels of Smac, Apaf-1, cytochrome c, caspase-9, and caspase-3 in MHCC97-H cells were determined via RT-PCR assays. As shown in Fig. 5, treatment with 30, 60, and 90 $\mu\text{g/mL}$ TF-SB significantly increased the mRNAs of Smac, Apaf-1, cytochrome c, caspase-9, and caspase-3 in MHCC97-H cells as compared with the control group ($P < 0.05$). Following TF-SB treatment for 48 h, Smac, Apaf-1, cytochrome c, caspase-

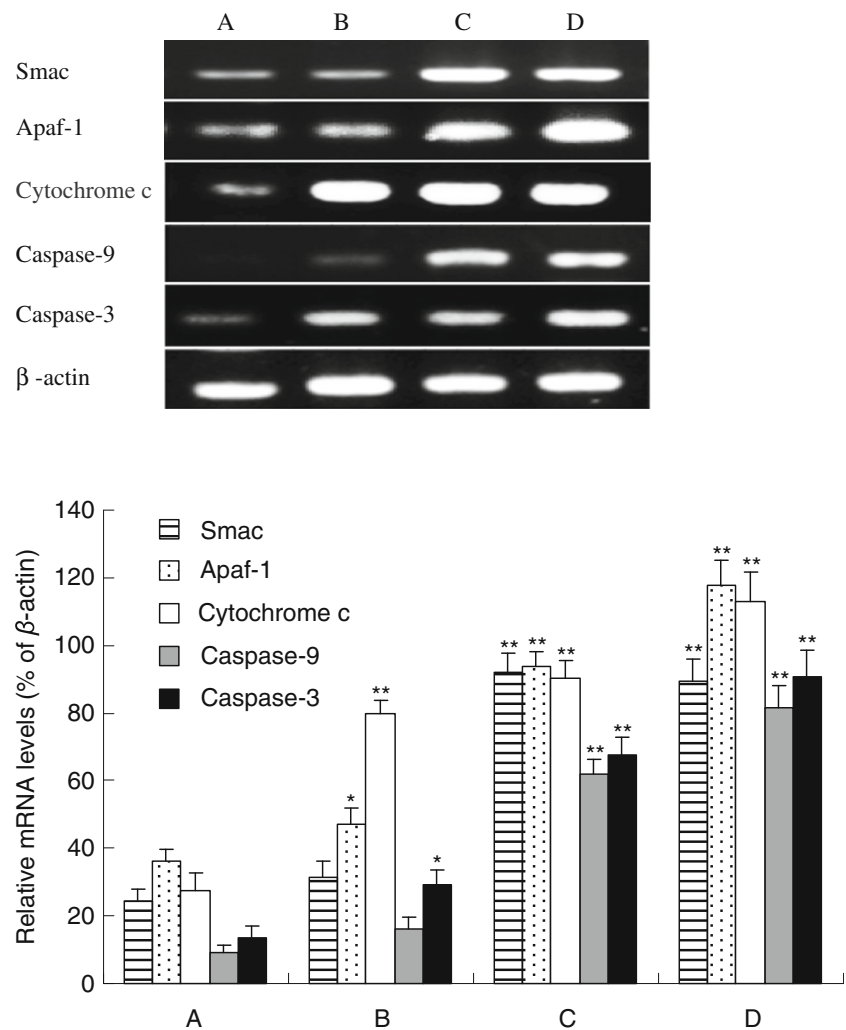
Fig. 5 The $\Delta\psi_m$ in MHCC97-H cells were observed by FCM after treatment with TF-SB. After treated with different concentrations of TF-SB for 48 h, the $\Delta\psi_m$ were observed by FCM with JC-1 probe staining. A control group, B 30 $\mu\text{g}/\text{mL}$ TF-SB group, C 60 $\mu\text{g}/\text{mL}$ TF-SB group, D 90 $\mu\text{g}/\text{mL}$ TF-SB group. Data are presented as the means \pm SEM from three independent experiments. * $P < 0.05$, ** $P < 0.01$ compared with the control group



9, and caspase-3 expression were upregulated in MHCC97-H cells. Furthermore, mRNAs of Smac, Apaf-1, cytochrome c, caspase-9, and caspase-3 in the 90 $\mu\text{g}/\text{mL}$

TF-SB group were increased by approximate 2.7-, 2.3-, 3.1-, 7.8-, and 5.6-fold. As shown in Fig. 6, it is showed that TF-SB markedly upregulated Smac, Apaf-1,

Fig. 6 The mRNA expression of Smac, Apaf-1, cytochrome c, caspase-9, and caspase-3 in MHCC97-H cells treated with different concentrations of TF-SB. After treatment with TF-SB for 48 h, mRNA levels were detected by RT-PCR analysis. This assay was done in quintuplicate. *A* control group, *B* 30 $\mu\text{g}/\text{mL}$ TF-SB group, *C* 60 $\mu\text{g}/\text{mL}$ TF-SB group, *D* 90 $\mu\text{g}/\text{mL}$ TF-SB group. Values represent means \pm SEM and were determined using the Student's *t* test. * $P < 0.05$, ** $P < 0.01$ compared with the control group



cytochrome c, caspase-9, and caspase-3 mRNA in a dose-dependent manner ($P < 0.05$).

Protein expression of Smac, Apaf-1, cytochrome c, caspase-9, and caspase-3 detected using Western blot analysis

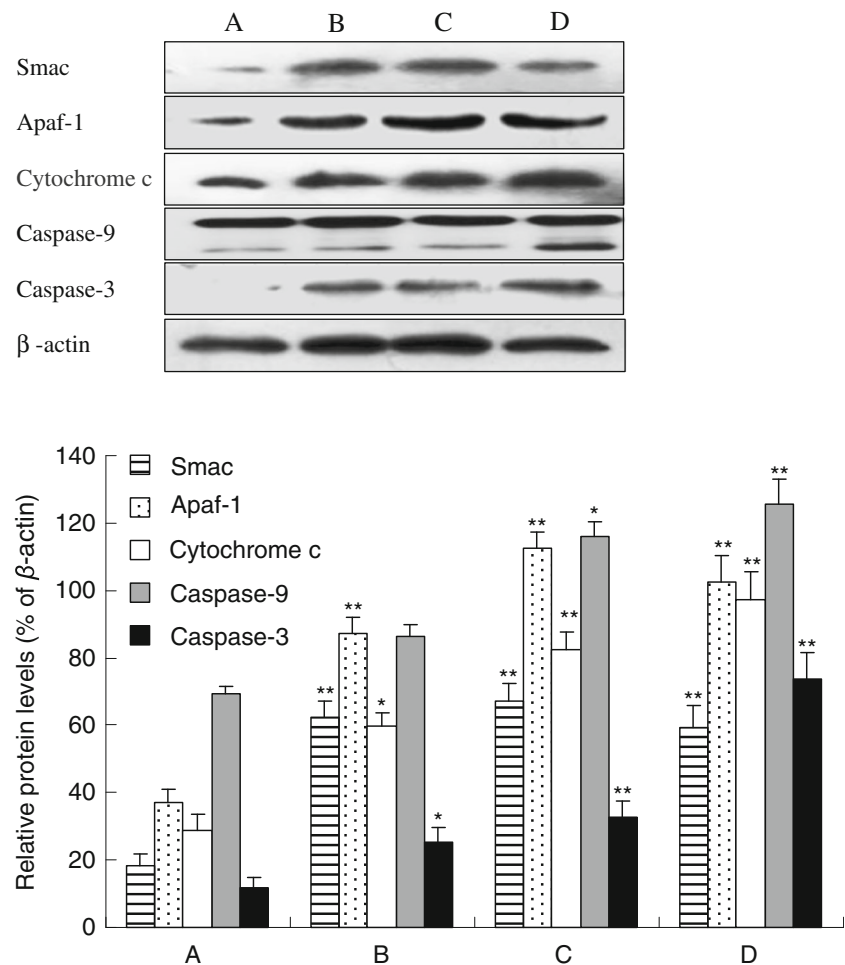
Based on the results of the RT-PCR, we further analyzed the effects of TF-SB on protein expression in MHCC97H cells. Smac, Apaf-1, cytochrome c, caspase-9, and caspase-3 protein were blotted against the corresponding antibodies as mentioned above in the MHCC97H cells after 48 h of treatment with TF-SB (0, 30, 60, and 90 $\mu\text{g}/\text{mL}$). As shown in Fig. 7, consistent with mRNA analysis, Western blot results showed that Smac, Apaf-1, cytochrome c, caspase-9, and caspase-3 increased after

TF-SB treatment. Furthermore, these effects were dose dependent ($P < 0.05$).

Discussion

Mitochondria are the center of the cellular metabolism and productivity, as well as an adjustable fulcrum of growth and death in cells. Recent studies have shown that the mitochondria play an essential role in cell apoptosis initiation. Mitochondrial proteins directly activate cellular apoptotic programs, which triggers a series of changes before cell death called the cell death cascade that eventually leads to apoptosis [25–27]. However, the mitochondrial pathway of apoptosis is very complex and is affected by a variety of protein regulatory

Fig. 7 The expression of Smac, Apaf-1, cytochrome c, caspase-9, and caspase-3 in MHCC97-H cells treated with concentration span of TF-SB. After treatment with TF-SB for 48 h, protein levels were detected by Western blot. This assay was done as triplicated. *A* control group, *B* 30 $\mu\text{g}/\text{mL}$ TF-SB group, *C* 60 $\mu\text{g}/\text{mL}$ TF-SB group, *D* 90 $\mu\text{g}/\text{mL}$ TF-SB group. Values represented means \pm SEM and were determined using the Student's *t* test. * $P < 0.05$, ** $P < 0.01$ compared with the control group



factors, including pro- and antiapoptotic factors. The imbalance in the apoptotic signal is closely related to the initiation of the apoptotic program [28, 29].

The signaling pathways activated by these stressors culminate in permeabilization of mitochondrial outer membrane and release of soluble proteins from the mitochondrial intermembrane space (IMS). Some soluble proteins including cytochrome c, which complexes with Apaf-1 and caspase-9 to form the apoptosome, released from the IMS have been able to trigger death by apoptosis. This results in activation of caspase-9, which orchestrates apoptosis by cleaving a subset of cellular substrates. Smac is a proapoptotic mitochondrial protein that is released from the mitochondria after apoptotic stimuli. It is combined with apoptosis inhibitor proteins BIR2 and BIR3, which activate caspase and induce apoptosis [30, 31]. The release of Smac into the cytosol from the mitochondrial inner membrane space is a key event in caspase-9 activation, which subsequently initiates a caspase cascade involving

caspase-3 [32]. These two proteins are involved in regulating the mitochondrial pathway of apoptosis. Studies suggested that the release of cytochrome c is the motivator for the mitochondria-initiated apoptosis. A considerable number of cytochrome c are released from the mitochondrion to the cytosol, which form the Apaf-1/cytochrome c complex with Apaf-1. The complex activates caspase-9, which catalyzes the formation of the terminal effector caspase-3 and subsequently leads to apoptosis [33, 34].

Previous studies have shown that the antitumor activity of CE-SB is associated to cell apoptosis [35]. In the HPLC analysis, TF-SB was mainly composed of scutellarin, apigenin, baicalein, and luteolin. Scutellarin could inhibit the growth of tongue cancer cells in vitro and regulate cell adhesion [36]. Apigenin could dose and time dependently repress the proliferation and clonogenic survival of the human breast cancer T47D and MDA-MB-231 cell lines [37]. Furthermore, apigenin has apoptosis- and autophagy-

inducing effects in cancer cells [37]. Zhu et al. [38] reported that apigenin could induce apoptosis and inhibit migration and invasion ability in T24 bladder cancer cells. Apigenin leads to apoptosis via PI3K/Akt pathway, regulation of Bcl-2 family, and activation of caspase-3 and PARP. Additionally, apigenin also causes G₂/M phase arrest [38]. Takahashi et al. [39] reported that baicalein induced apoptosis through a caspase-dependent pathway in pancreatic cancer cells. The proapoptotic effect of baicalein is mediated through reducing the expression of the prosurvival protein Mcl-1 [39]. Moreover, baicalein could inhibit tumor cell invasion and metastasis via the suppression of the ERK pathway [40].

In our study, TF-SB significantly inhibited the proliferation of MHCC97-H cells in a dose- and time-dependent manner, as indicated by MTT assay. This is consistent with our previous findings, wherein CE-SB inhibited the proliferation of hepatoma H22 cells [41]. Then, we detected the apoptosis rate by the double-staining of annexin V-FITC and PI in MHCC97-H cells. After treatment with different TF-SB concentrations, the apoptotic rate increased with increasing TF-SB concentration. The degradation of DNA fragments gradually increased with increasing TF-SB concentration. Furthermore, DNA ladder analyses clearly revealed a typical ladder tape in the 90 µg/mL TF-SB group after 48 h. Thus, TF-SB induced apoptosis of MHCC97-H cells with DNA degradation. The loss of $\Delta\psi_m$ and cytochrome C release triggers apoptosis. After treatment with different TF-SB concentrations, the loss of $\Delta\psi_m$ increased in a dose-dependent manner. Therefore, TF-SB induces changes in $\Delta\psi_m$.

To further investigate the molecular mechanism of TF-SB-induced apoptosis, we observed the mRNA and protein expression of Smac, Apaf-1, caspase-9, survivin via semiquantitative RT-PCR, and Western blot analysis. The results show that the expression of Smac, Apaf-1, cytochrome c, caspase-9 and caspase-3 were upregulated. These results suggest that TF-SB induces apoptosis in MHCC97-H cells. The mechanism may be related to the upregulation of Smac, Apaf-1, cytochrome c, caspase-9, and caspase-3.

Conclusion

In conclusion, TF-SB induces apoptosis in HCC cell line MHCC97-H in vitro. $\Delta\psi_m$ decreases simultaneously with increasing TF-SB concentration. This effect may be associated with the expressions of Smac, Apaf-1, cytochrome c, caspase-9, and caspase-3, which are greatly dependent on the mitochondrial pathway of apoptosis.

Acknowledgments This study was supported by National Natural Science Foundation of China, no. 81102711; the Fundamental Research Funds for the Central Universities, China, no. xjj2011039; and Sci-Tech Program of Administration of Traditional Chinese Medicine of Shaanxi Province, China, no. 13-JC005.

Conflicts of interest None

References

- Jemal A, Bray F, Center MM, Ferlay J, Ward E, Forman D. Global cancer statistics. *CA Cancer J Clin*. 2011;61:69–90.
- Chen P, Hu MD, Deng XF, Li B. Genistein reinforces the inhibitory effect of Cisplatin on liver cancer recurrence and metastasis after curative hepatectomy. *Asian Pac J Cancer Prev*. 2013;14:759–64.
- Marrero JA. Multidisciplinary management of hepatocellular carcinoma: where are we today? *Semin Liver Dis*. 2013;33:S3–S10.
- Ali R, Mirza Z, Ashraf GM, Kamal MA, Ansari SA, et al. New anticancer agents: recent developments in tumor therapy. *Anticancer Res*. 2012;32:2999–3005.
- Gotoh H, Sears JE, Eschenmoser A, Boger DL. New insights into the mechanism and an expanded scope of the Fe(III)-mediated vinblastine coupling reaction. *J Am Chem Soc*. 2012;134:13240–3.
- Namdeo A, Sharma A. HPLC analysis of camptothecin content in various parts of *Nothapodytes foetida* collected on different periods. *Asian Pac J Trop Biomed*. 2012;2:389–93.
- Dai ZJ, Tang W, Lu WF, Gao J, Kang HF, Ma XB, et al. Antiproliferative and apoptotic effects of β -elemene on human hepatoma HepG2 cells. *Cancer Cell Int*. 2013;13:27.
- Dai ZJ, Wang XJ, Li ZF, Ji ZZ, Ren HT, Tang W, et al. *Scutellaria barbata* extract induces apoptosis of hepatoma H22 cells via the mitochondrial pathway involving caspase-3. *World J Gastroenterol*. 2008;14:7321–8.
- Chen BD, Ning ML, Zhou WY, Zou LL, Yu SN. Antitumor effects of *Scutellaria barbata* ethanol extracts in mice transplanted with human hepatocellular carcinoma (HepG2) cells. *Afr J Pharm Pharmacol*. 2011;5:1553–7.
- Goh D, Lee YH, Ong ES. Inhibitory effects of a chemically standardized extract from *Scutellaria barbata* in human colon cancer cell lines, LoVo. *J Agric Food Chem*. 2005;53:8197–204.
- Yin X, Zhou J, Jie C, Xing D, Zhang Y. Anticancer activity and mechanism of *Scutellaria barbata* extract on human lung cancer cell line A549. *Life Sci*. 2004;75:2233–44.
- Perez AT, Arun B, Tripathy D, Tagliaferri MA, Shaw HS, Kimmick GG, et al. A phase 1B dose escalation trial of *Scutellaria barbata* (BZL101) for patients with metastatic breast cancer. *Breast Cancer Res Treat*. 2010;120:111–8.
- Chen Y, Xu SS, Chen JW, Wang Y, Xu HQ, Fan NB, et al. Anti-tumor activity of *Annona squamosa* seeds extract containing annonaceous acetogenin compounds. *J Ethnopharmacol*. 2012;142:462–6.
- Kalimuthu S, Se-Kwon K. Cell survival and apoptosis signaling as therapeutic target for cancer: marine bioactive compounds. *Int J Mol Sci*. 2013;14:2334–54.
- Yoo KH, Park JH, Lee DK, Fu YY, Baek NI, Chung IS. Pomolic acid induces apoptosis in SK-OV-3 human ovarian adenocarcinoma cells through the mitochondrial-mediated intrinsic and death receptor-induced extrinsic pathways. *Oncol Lett*. 2013;5:386–90.

16. Delivani P, Martin SJ. Mitochondrial membrane remodeling in apoptosis: an inside story. *Cell Death Differ*. 2006;13:2007–10.
17. Xu YY, You YW, Ren XH, Ding Y, Cao J, Zang WD, et al. Endoplasmic reticulum stress-mediated signaling pathway of gastric cancer apoptosis. *Hepatogastroenterology*. 2012;59:2377–84.
18. Niu CC, Lin SS, Yuan LJ, Chen LH, Wang IC, Tsai TT, et al. Hyperbaric oxygen treatment suppresses MAPK signaling and mitochondrial apoptotic pathway in degenerated human intervertebral disc cells. *J Orthop Res*. 2013;31:204–9.
19. Culbreth ME, Harill JA, Freudenrich TM, Mundy WR, Shafer TJ. Comparison of chemical-induced changes in proliferation and apoptosis in human and mouse neuroprogenitor cells. *Neurotoxicology*. 2012;33:1499–510.
20. Song Y, Xia Z, Shen K, Zhai X. Autocatalytic caspase-3 driven by human telomerase reverse transcriptase promoter suppresses human ovarian carcinoma growth in vitro and in mice. *Int J Gynecol Cancer*. 2013;23:642–9.
21. Dai ZJ, Lu WF, Gao J, Kang HF, Ma YG, Zhang SQ, et al. Anti-angiogenic effect of the total flavonoids in *Scutellaria barbata* D. Don. *BMC Complement Altern Med*. 2013;13:150.
22. Yuan X, Zhang B, Gan L, Wang ZH, Yu BC, Liu LL, et al. Involvement of the mitochondrion-dependent and the endoplasmic reticulum stress signaling pathways in isoliquiritigenin-induced apoptosis of HeLa cell. *Biomed Environ Sci*. 2013;26:268–76.
23. Qin S, Yang C, Li S, Xu C, Zhao Y, Ren H. Smac: its role in apoptosis induction and use in lung cancer diagnosis and treatment. *Cancer Lett*. 2012;318:9–13.
24. Ferraro E, Pesaresi MG, De Zio D, Cencioni MT, Gortat A, Cozzolino M, et al. Apaf1 plays a pro-survival role by regulating centrosome morphology and function. *J Cell Sci*. 2011;124:3450–63.
25. Loureiro R, Mesquita KA, Oliveira PJ, Vega-Naredo I. Mitochondria in cancer stem cells: a target for therapy. *Recent Pat Endocr Metab Immune Drug Discov*. 2013;7:102–14.
26. Lee HH, Park C, Jeong JW, Kim MJ, Seo MJ, Kang BW, et al. Apoptosis induction of human prostate carcinoma cells by cordycepin through reactive oxygen species mediated mitochondrial death pathway. *Int J Oncol*. 2013;42:1036–44.
27. Fang XY, Chen W, Fan JT, Song R, Wang L, Gu YH, et al. Plant cyclopeptide RA-V kills human breast cancer cells by inducing mitochondria-mediated apoptosis through blocking PDK1-AKT interaction. *Toxicol Appl Pharmacol*. 2013;267:95–103.
28. Guerrero AD, Schmitz I, Chen M, Wang J. Promotion of caspase activation by caspase-9 mediated feedback amplification of mitochondrial damage. *J Clin Cell Immunol*. 2012;3(3):1000126.
29. Platini F, Pérez-Tomás R, Ambrosio S, Tessitore L. Understanding autophagy in cell death control. *Curr Pharm Des*. 2010;16:101–13.
30. Roberts DL, Merrison W, MacFarlane M, Cohen GM. The inhibitor of apoptosis protein-binding domain of Smac is not essential for its proapoptotic activity. *J Cell Biol*. 2001;153:221–8.
31. Ng H, Smith DJ, Nagley P. Application of flow cytometry to determine differential redistribution of cytochrome c and Smac/DIABLO from mitochondria during cell death signaling. *PLoS One*. 2012;7:e42298.
32. Du C, Fang M, Li Y, Li L, Wang X. Smac, a mitochondrial protein that promotes cytochrome c-dependent caspase activation by eliminating IAP inhibition. *Cell*. 2000;102:33–42.
33. Sun KW, Ma YY, Guan TP, Xia YJ, Shao CM, Chen LG, et al. Oridonin induces apoptosis in gastric cancer through Apaf-1, cytochrome c and caspase-3 signaling pathway. *World J Gastroenterol*. 2012;18:7166–74.
34. Chao Y, Shiozaki EN, Srinivasula SM, Rigotti DJ, Fairman R, Shi Y. Engineering a dimeric caspase-9: a re-evaluation of the induced proximity model for caspase activation. *PLoS Biol*. 2005;3:e183.
35. Lee TK, Lee YJ, Kim DI, Kim HM, Chang YC, Kim CH. Pharmacological activity in growth inhibition and apoptosis of cultured human leiomyoma cells of tropical plant *Scutellaria barbata* D. Don (Lamiaceae). *Environ Toxicol Pharmacol*. 2006;21:70–9.
36. Li H, Huang D, Gao Z, Lv Y, Zhang L, Cui H, et al. Scutellarin inhibits cell migration by regulating production of $\alpha\text{v}\beta\text{6}$ integrin and E-cadherin in human tongue cancer cells. *Oncol Rep*. 2010;24(5):1153–60.
37. Cao X, Liu B, Cao W, Zhang W, Zhang F, Zhao H, et al. Autophagy inhibition enhances apigenin-induced apoptosis in human breast cancer cells. *Chin J Cancer Res*. 2013;25(2):212–22.
38. Zhu Y, Mao Y, Chen H, Lin Y, Hu Z, Wu J, et al. Apigenin promotes apoptosis, inhibits invasion and induces cell cycle arrest of T24 human bladder cancer cells. *Cancer Cell Int*. 2013;13(1):54.
39. Takahashi H, Chen MC, Pham H, Angst E, King JC, Park J, et al. Baicalein, a component of *Scutellaria baicalensis*, induces apoptosis by Mcl-1 down-regulation in human pancreatic cancer cells. *Biochim Biophys Acta*. 2011;1813(8):1465–74.
40. Chen K, Zhang S, Ji Y, Li J, An P, Ren H, et al. Baicalein inhibits the invasion and metastatic capabilities of hepatocellular carcinoma cells via down-regulation of the ERK pathway. *PLoS One*. 2013;8(9):e72927.
41. Dai ZJ, Gao J, Li ZF, Ji ZZ, Kang HF, Guan HT, et al. In vitro and in vivo antitumor activity of *Scutellaria barbata* extract on murine liver cancer. *Molecules*. 2011;16:4389–400.